# Neural cell adhesion molecule is a cardioprotective factor up-regulated by metabolic stress.

AUTHOR(S):

Nagao, Kazuya; Ono, Koh; Iwanaga, Yoshitaka; Tamaki, Yodo; Kojima, Yoji; Horie, Takahiro; Nishi, Hitoo; ... Hasegawa, Koji; Kita, Toru; Kimura, Takeshi

CITATION:

Nagao, Kazuya ...[et al]. Neural cell adhesion molecule is a cardioprotective factor up-regulated by metabolic stress.. Journal of molecular and cellular cardiology 2010, 48(6): 1157-1168

ISSUE DATE:

2010-06

URL:

http://hdl.handle.net/2433/123422

# Neural cell adhesion molecule is a cardioprotective factor up-regulated by metabolic stress

**Kazuya Nagao[1], Koh Ono[1], Yoshitaka Iwanaga[2], Yodo Tamaki[1], Yoji Kojima[1], Takahiro Horie[1], Hitoo Nishi[1], Minako Kinoshita[1], Yasuhide Kuwabara[1], Koji Hasegawa[3], Toru Kita[4], and Takeshi Kimura[1]**

[1]Department of Cardiovascular Medicine, Graduate School of Medicine, Kyoto University, Kyoto, Japan; [2]Department of Cardiovascular Medicine, Graduate School of Medicine, Kinki University, Osaka, Japan; [3]Division of Translational Research, Kyoto Medical Center, National Hospital Organization, Kyoto, Japan; [4]Kobe City Medical Center General Hospital, Hyogo, Japan

**Address for correspondence:**

Koh Ono, MD, PhD,

Department of Cardiovascular Medicine, Kyoto University,

54 Shogoin-Kawaharacho, Sakyo-ku, Kyoto, 606-8507, Japan

Tel: +81-75-751-3190

Fax: +81-75-751-3203

E-mail: kohono@kuhp.kyoto-u.ac.jp

Subtitle: NCAM protects cardiomyocytes following metabolic stress

**Abstract**

Screening for cell-surface proteins up-regulated under stress conditions may lead to the identification of new therapeutic targets. To search for genes whose expression was enhanced by treatment with oligomycin, a mitochondrial-$F_0F_1$ ATP synthase inhibitor, signal sequence trapping was performed in H9C2 rat cardiac myoblasts. One of the genes identified was that for neural cell adhesion molecule (NCAM, CD56), a major regulator of development, cell survival, migration, and neurite outgrowth in the nervous system. Immunohistochemical analyses in a mouse myocardial infarction model revealed that NCAM was strongly expressed in residual cardiac myocytes in the infarcted region. Increased expression of NCAM was also found during the remodeling period in a rat model of hypertension-induced heart failure. Lentivirus-mediated knockdown of NCAM decreased the cell growth and survival following oligomycin treatment in H9C2 cells. In primary rat neonatal cardiac myocytes, NCAM was also found to be up-regulated and played a protective role following oligomycin treatment. Analyses of downstream signaling revealed that knockdown of NCAM significantly decreased the basal AKT phosphorylation level. In contrast, NCAM-mimetic peptide P2d activated AKT and significantly reduced

oligomycin-induced cardiomyocyte death, which was abolished by treatment with the PI3K inhibitor LY-294002 as well as overexpression of the dominant-negative AKT mutant. These findings demonstrate that NCAM is a cardioprotective factor up-regulated under metabolic stress in cardiomyocytes and augmentation of this signal improved survival.

# 1. Introduction

It is generally regarded that following chronic pressure and volume overload and after regional myocardial infarction (MI), the heart gradually develops a diminished capacity to generate adenosine triphosphate (ATP) required for the heart to maintain cardiac output at an adequate level [1-3]. Consistent with this, reductions in tissue content and the activity of complexes I-IV of the mitochondrial respiratory chain have been reported in animal models of cardiac failure and in end-stage human failing hearts [4-6].

A growing body of evidence shows that as a response to various pathological conditions, the heart produces membrane and/or secretes factors to maintain its performance in heart failure [7-10]. In order to find membrane and/or secretes factors up-regulated under metabolic stress, a signal sequence trapping (SST) method, a general strategy for cloning secreted proteins and type I membrane proteins, was applied using a U3Ceo vector in H9C2 rat cardiac myoblasts in combination with a functional cloning method with oligomycin, a mitochondrial-$F_0F_1$ ATP synthase inhibitor [11].

One of the genes identified was that for neural cell adhesion molecule (NCAM, CD56), a major regulator of development, cell survival, migration, and neurite outgrowth in the

nervous system [12, 13]. Homophilic and heterophilic NCAM binding result in the activation of a number of signaling cascades, which in turn result in context-dependent biological responses in neuronal cells [14-16]. However, the biological function of NCAM in cardiac myocytes remains unknown.

Here, it is reported that (1) NCAM is a type I membrane protein identified by SST in H9C2 cardiomyoblasts induced by oligomycin treatment, (2) NCAM was up-regulated in a mouse MI model and during the remodeling period of hypertrophy to heart failure in a Dahl salt-sensitive rat model, (3) endogenous NCAM contributed to AKT activity and protected cardiac myocytes from cell death induced by oligomycin-induced metabolic stress, and (4) treatment with NCAM mimetic peptide P2d activated AKT and improved the cardiomyocyte survival rate against metabolic stress.

## 2. Materials and methods

### *2.1. Reagents*

Oligomycin, SB202190, SP600125, and LY294004 were purchased from Calbiochem. The P2d and scrambled P2d (scrP2d) peptides were generous gifts from Professor Elisabeth Bock (Panum Institute, University of Copenhagen, Copenhagen, Denmark) and STEMCELL Technologies Inc.(Vancouver, BC, Canada).

### *2.2. Cell culture*

The rat myocyte cell line H9C2 was obtained from the American Type Culture Collection (Rockville, MD, USA) and maintained in DMEM supplemented with 10% fetal bovine serum (FBS). Isolation of primary neonatal rat ventricular cardiomyocytes was carried out using an established procedure as described previously [17] and cultured in medium containing 10% FBS.

### *2.3. Plasmid and cell infection*

The U3Ceo retroviral vector was a gift from Harald von Melchner (University of

Frankfurt Medical School). Viruses were produced at 32°C, and virus-containing medium was collected 24 h post-transfection and filtered through a 0.45 μm filter. H9C2 cells were plated in six-well plates at a density of $5\times10^5$ cells/well. One round of retroviral infection was performed by replacing the medium with 2 mL of U3Ceo virus (containing 8 μg/mL of Polybrene, Sigma-Aldrich), followed by centrifugation of the six-well plates at 1220×g for 30 min at 32°C. Stably transfected clones were selected in normal growth medium with the addition of G-418 (1 mg/mL).

The oligonucleotide used for small interfering RNA (siRNA) of NCAM was NCAM-siRNA: sense 5' GGCAGGAGATGCCAAAGAT-3'. The siRNA construct was made using a pSINsi-mU6 vector (Takara Bio., Inc.). siRNA and the dominant negative form of rat AKT1 (AKT-AA: T308A/S473A) [18] was introduced into the lentivirus vector plasmid pLenti6/V5-D-TOPO vector (Invitrogen) and transduced into cardiac myocytes as was done for retroviral infection.

*2.4. Flow Cytometry*

After the indicated treatments, the cells were washed quickly and suspended in 50 μL PBS and incubated for 30 min at 4°C with 5 μL of FITC conjugated CD2 (Leu-5b). Cells

were washed 3 times with PBS, suspended in 500 μL PBS, and analyzed using a FACS Aria (BD Biosciences) with FITC-specific settings.

*2.5. 5'-RACE*

5'-RACE was performed with 5 μg of total RNA using a 5'RACE System for Rapid amplification of cDNA Ends, version 2.0 (Invitrogen), in accordance with the manufacturer's instructions. CD2 specific primers were 5'-CAAGTTGATGTCCTGACCCAAG-3' and 5'-GGTTTCCAAGGCATTCGTAATCTC-3'. The amplification of tailed cDNA was performed using 35 cycles of 94°C for 1 min, 55°C for 1 min, and 72°C for 2 min.

*2.6. Western blotting*

For NCAM assays, a polyclonal rabbit anti-rat NCAM antibody (diluted 1:5000; a generous gift from Professor Elisabeth Bock,) was used as the primary antibody, and an anti-rabbit Ig peroxidase conjugate (whole molecule conjugate; diluted 1:2000; Sigma) as the secondary antibody. An anti-β-actin antibody (diluted 1:3000; Sigma) was used as a loading control. Anti-phosphospecific p38 (diluted 1:250), anti-phosphospecific AKT

(Ser473) (diluted 1:1000), anti-total AKT (diluted 1:500) and anti-phosphospecific JNK antibodies (diluted 1:500) were obtained from Cell Signaling. Anti-phosphospecific ERK 1/2 (diluted 1:500), anti-total ERK 1/2 (diluted 1:500), anti-total p38 (diluted 1:200) and anti-total JNK (diluted 1:500) was obtained from Santa cruz.

*2.7. Real-time PCR*

For real-time PCR, the reaction was performed using a SYBR Green PCR master mix (Applied Biosystems), and the products were analyzed using a thermal cycler (ABI Prism 7900HT sequence detection system). The levels of GAPDH transcripts were used to normalize cDNA levels.

Gene-specific primers were as follows:

rat NCAM sense, 5’ AATCAGCGTTGGAGAGTCCA-3’,

antisense, 5’ CGTCTTCAGCGGTGACCA-3’,

mouse NCAM sense, 5’ ACAGAAACCCGTGGAGATG-3’,

antisense, 5’ GTCTCTGTGGCTCTCGTTCC-3’

(these primers recognized all forms of NCAM splicing variants) ;

rat ANF sense, 5’ CGTGCCCCGACCCACGCCAGCATGGGCTCC-3’,

antisense, 5’ GGCTCCGAGGGCCAGCGAGCAGAGCCCTCA-3’; and

GAPDH sense, 5’ TTGCCATCAACGACCCCTTC-3’,

antisense, 5’ TTGTCATGGATGACCTTGGC-3’.

*2.8. ATP measurement*

Intracellular ATP concentration was measured using an ATP bioluminescence assay kit (TOYO ink) in accordance with the manufacturer’s protocol and the data was normalized for total cell protein.

*2.9. Cell proliferation assay and BrdU uptake*

H9C2 cells transfected with either control-siRNA or with NCAM-siRNA, were plated at $1.2\times10^4$/mL into 10 cm dishes and cultured in DMEM containing 10% FBS. The number of H9C2 cells was counted using a cell counter (COULTER particle counter, GMI). BrdU uptake by H9C2 cells was quantified using a BrdU Labeling and Detection Kit III as described by the manufacturer (Roche Diagnostics).

*2.10. MTT assay*

Quantitative determination of viable cells was performed using an MTT assay. Briefly, the cells were labeled with MTT (Thiazolyl Blue Tetrazolium Bromide, Sigma) at a final concentration of 0.5 mg/mL for at least 4 h at 37°C. Viability was then evaluated by measuring the absorbance at 595 nm using an Elx800 Microplate Reader (BIO-TEK Instruments Inc.).

*2.11. Two-color fluorescence cell viability assay*

Simultaneous determination of live and dead cells was performed using a LIVE/DEAD Viability/Cytotoxicity Assay Kit (Invitrogen). Briefly, after the indicated treatments, cells were labeled with calcein AM (2 μM) and ethidium homodimer-1 (4 μM) probes, which are specific for intracellular esterase activity and membrane integrity, respectively. The number of live cells (labeled green) and dead cells (labeled red) was counted in 15 random microscopic fields (×100) per experiment using a fluorescence microscope. The ratio of live cells (green/ green+ red) was calculated and used to determine the cell viability (%).

*2.12. Animal Tissue*

The investigation conformed with the *Guide for the Care and Use of Laboratory Animals*

published by the National Institutes of Health (NIH Publication No. 85-23, Revised 1996), and was approved by the Institutional Animal Research Committee of Kyoto University. In experiments using an MI model mouse, C57/BL6 mice were anesthetized with 0.5% pentobarbital (Dainippon Sumitomo Pharma), and open-chest coronary artery ligation was performed. MI was induced by ligating the left anterior descending coronary artery. In sham-operated mice, open-chest surgery was performed without coronary artery ligation. At the indicated number of days after surgery (n=3 per group), hearts were isolated for immunohistochemical and real-time PCR analyses. In experiments using Dahl salt-sensitive (DS) rats, male DS rats were fed an 8% NaCl (high-salt) diet after the age of 6 weeks. The animals were sacrificed at the LVH (11 weeks) and CHF (17 weeks) stages. DS rats that were fed a low-salt (0.5% NaCl) diet and remained normotensive and were used as age-matched controls.

*2.13. Immunohistochemistry*

Immunohistochemical staining was performed using a conventional (ABC) method. Briefly, incubation and washing procedures were carried out at room temperature. After deparaffinization and antigen retrieval, endogeneous peroxidase activity was blocked using

0.3% $H_2O_2$ in methylalcohol for 30 min. The glass slides were washed in PBS (6 times, 5 min each) and mounted with 1% normal serum in PBS for 30 min. Subsequently anti-NCAM rabbit polyclonal antibody H-300 (Santa Cruz) diluted to 1:100 in PBS was applied overnight at 4°C. The slides were incubated with biotinylated anti-rabbit serum (second antibody) diluted to 1:300 in PBS for 40 min, followed by washes in PBS (6 times, 5 min each). Avidin-biotin-peroxidase complex (ABC) (ABC-Elite, Vector Laboratories) at a dilution of 1:100 in PBS was applied for 50 min. After washing in PBS (6 times, 5 min each), the detection reaction was carried out with DAB, and nuclei were counterstained with hematoxylin.

*2.14. Statistics*

Data are presented as means±SEM. Statistical significance ($P<0.05$) was determined between groups using an ANOVA followed by Tukey's Multiple Comparison Test for multiple groups or a Student’s t-test for two groups.

## 3. Results

### *3.1. NCAM was identified to be up-regulated under metabolic stress in H9C2 cells*

Oligomycin, a specific blocker of mitochondrial-$F_0F_1$ ATP synthase, was used to induce metabolic stress. Treatment of H9C2 cells with 20 μM oligomycin for 48 h significantly decreased the cellular ATP concentration (Fig. 1A).

In order to identify the genes of secreted proteins and type I membrane proteins up-regulated under metabolic stress, SST method in combination with a functional screening was performed, using the U3Ceo vector [11] in H9C2 rat cardiac myoblasts. An overview of the experimental procedure is indicated in Fig. 1B. In the U3Ceo vector, human CD2 cell antigen/neomycin-phosphotransferase fusion gene (Ceo) is inserted into the 3'-long terminal repeat (LTR). After U3Ceo retroviral infection, proviral integrations into the introns of expressed genes in the target cells result in splicing of exons upstream to Ceo, leading to cell-provirus fusion transcription. If these exons possess a signal sequence, it enables fusion protein transport to the cell membrane and makes the cells CD2 positive and G418 resistant. After U3Ceo retroviral infection, CD2 expression was estimated by flow cytometry and CD2-negative cells were collected and expanded for the next

experiment (Fig. 1B, 1st sorting, red). After oligomycin treatment, a small portion of cells treated with oligomycin became CD2 positive (Fig. 1B, 2nd sorting, blue). These CD2-positive cells were collected and expanded in complete growth medium to form single clones. Samples from each clone were collected and analyzed to determine the identity of the inserted genes. The fused mRNA of U3Ceo and an endogenous gene in oligomycin-treated CD2-positive cells was amplified by 5' rapid amplification of cDNA ends (5'-RACE). In one of the clones obtained, the junctional sequence of the fused cDNA revealed that viral insertion occurred at the 3' end of exon 1 of the NCAM gene (Fig. 1C).

To ensure that CD2 expression was truly regulated by oligomycin treatment, the pattern of CD2 expression was examined in this clone. Flow cytometry analysis revealed that treatment with oligomycin for 48 h induced cell surface CD2 expression (Fig. 1D). This effect was concentration- and time-dependent (Fig. 1E). In this clone, endogenous NCAM was truncated by the insertion of U3Ceo, and the fusion protein might be expressed in a different way from intact NCAM. Thus, the level of endogenous NCAM expression was analyzed in H9C2 cells. Real-time PCR analysis showed that significant up-regulation of NCAM mRNA expression was observed at 48 h after treatment with oligomycin (Fig. 1F). Western blotting revealed that H9C2 cells expressed NCAM 120 and 140 with NCAM 140

predominating under basal conditions. Oligomycin treatment up-regulated NCAM 140, while the expression of NCAM 120 was unchanged. (Fig. 1G).

*3.2. Histological examination in a mouse model of myocardial infarction*

Next, the expression pattern of NCAM in the hearts was analyzed. Myocardial ischemia is a typical model of metabolic stress in the diseased heart. Thus, the expression of NCAM in a mouse model of MI was examined. The expression levels of NCAM in sham-operated (n=3) and MI mice (n=4) were determined by real time PCR analysis. Apex in an MI mouse indicates an infarcted area and septum in an MI mouse indicates a non-infacted area. Significant NCAM up-regulation was observed in infracted areas at 7 days after surgery (Fig. 2A). By immunohistochemistry, staining of NCAM in control mice was only observed in the intercalated discs (Fig. 2B and C). However, in the MI model, strong staining was observed in the myocardium adjacent to the infarcted area (Fig. 2D and E); whereas, staining was restricted to the intercalated disks in remote areas (Fig. 2F). Even in the chronic phase at 12 months after surgery, strong NCAM staining was still detected in residual myocytes in the scared fibrotic area (Fig. 2G).

*3.3. Histological examination in a rat model of heart failure*

Load-induced hypertrophy triggers metabolic stress, leading to pathological remodeling and heart failure [1-3]. To examine the change in NCAM expression pattern during this process, a rat model of hypertension-induced heart failure was analyzed. In Dahl salt-sensitive (DS) rats on a high-salt diet, systemic hypertension caused compensated concentric left ventricular hypertrophy (LVH stage) at the age of 11 weeks, followed by marked LV dilatation and global hypokinesis at 17 weeks (CHF stage) [19-21]. Fig. 3A indicates that the ANF expression level increased in the LV of DS rats at the LVH and CHF stages, as determined by real-time PCR analyses, while the ANF expression levels were unchanged in the LV of control rats, which were fed on a low salt (0.5% NaCl) diet.

Immunohistochemical staining of NCAM in DS rats was performed. Similar to the mouse model, the staining in the control rats at the age of 11 weeks was very weak and restricted to the intercalated discs (Fig. 3B and Fig. 3C). However, at the LVH stage of DS rats fed on a high-salt diet, a strong and heterogeneous expression pattern of NCAM staining was observed. As shown in Fig. 3D-3H, NCAM was mainly expressed in the endo- and subendo-cardium facing the ventricular cavity, whereas its expression was very weak in the subepicardial area. To further analyze the distribution pattern of NCAM staining,

Masson's Trichrome staining was performed, and it was revealed that the myocardium surrounding the fibrotic area (arrows in Fig. 3I) had intense staining of NCAM (arrowheads in Fig. 3J. Fig. 3I and J are the sequential section) at the LVH stage.

At the CHF stage, strong NCAM staining was observed throughout the myocardium (Fig. 3K and 3L). Fig. 3M is the staining of NCAM in control rats at the age of 17 weeks.

The NCAM levels in the LV of DS rats at LVH and CHF periods were quantified by real-time PCR analyses and western blotting analysis (Fig. 3N and O). Consistent with the results of immunohistochemical analyses, both mRNA and protein of NCAM expression levels were enhanced in the LVH stage, and significant and strong expression was observed in CHF stage.

### *3.4. Knockdown of NCAM reduced proliferation of H9C2 cells and reduced the survival rate following oligomycin treatment*

To investigate the function of NCAM in cardiac myocytes, an siRNA construct directed against NCAM was generated and introduced by lentivirus, leading to an effective decrease in the expression of both NCAM120 and 140 in H9C2 cells (Fig. 4A). Interestingly, transfection of H9C2 cells with NCAM-siRNA was found to decrease their proliferation

rate (Fig. 4B). In consistent with this, the uptake of 5-bromo-2'-deoxyuridine (BrdU) was also decreased by the knockdown of NCAM (Fig. 4C), indicating that endogenous NCAM played a significant role in H9C2 cell proliferation.

Next, H9C2 cells transfected with control-siRNA or NCAM-siRNA vector were treated with oligomycin for 48 h, and the role of NCAM in cell survival under metabolic stress was evaluated. As shown in Fig. 4D, oligomycin treatment induced severe cell shrinkage when NCAM was knocked down. Consistent with the reduction in the proliferation rate, the MTT level was significantly reduced in NCAM-knocked down H9C2 cells under basal conditions and decreased further after oligomycin treatment (Fig. 4E).

To further confirm that NCAM protects against oligomycin-induced metabolic stress, simultaneous determination of live and dead cells was performed. Under basal conditions, although the number of viable cells was decreased when NCAM was knocked-down (Fig. 4G main graph, siCTRL oligomycin- vs. siNCAM oligomycin-), this was mainly due to a decrease in the proliferation rate and not to cell death, since no significant increase in dead cells was observed in this group (Fig. 4G main graph, siCTRL oligomycin- vs. siNCAM oligomycin-). Indeed, when cell viability (live cells (green)/total cells (green+red)) was determined in each group, more than 99% of H9C2 cells were found to be viable in both

control and NCAM-knocked-down H9C2 cells (Fig. 4G inset, siCTRL oligomycin- and siNCAM oligomycin-). Although the number of viable cells was decreased by oligomycin treatment in control-siRNA transfected H9C2 cells (Fig. 4G main graph, siCTRL oligomycin- vs. siCTRL oligomycin+), this was mainly due to a decrease in cell growth and not to enhanced cell death, since nearly 90% of cells were shown to be alive (Fig. 4G inset, siCTRL oligomycin+). However, treatment with oligomycin in NCAM-knocked-down H9C2 cells resulted in increased cell death, which in turn led to less than 50% cell viability (Fig. 4G main graph and inset, siNCAM oligomycin+).

These results suggest that endogenous NCAM plays a significant role in protecting against metabolic stress as well as in cell proliferation in H9C2 cells.

*3.5. Expression and protective function of NCAM in primary rat neonatal cardiac myocytes*

The expression and function of NCAM during metabolic stress was also analyzed in primary rat neonatal cardiac myocytes. Because primary rat neonatal cardiac myocytes were more susceptible to metabolic stress, treatment with low concentration of 0.1 μM oligomycin for 48h significantly reduced the intracellular ATP concentration (Fig. 5A). Treatment with oligomycin rapidly activated stress responsive MAPK p38, while JNK was

not activated (Fig. 5B). A significant up-regulation of NCAM mRNA was observed at 48 h after treatment with oligomycin (Fig. 5C). Western blotting analysis showed that, similar to H9C2 cells, primary rat neonatal cardiac myocytes expressed NCAM 120 and 140, and that both variants were up-regulated by oligomycin treatment (Fig. 5D).

To determine whether the activation of MAPK might be responsible for the up-regulation of NCAM under metabolic stress, cells were treated with the p38 inhibitor SB202190 or the JNK inhibitor SP600125 and the expression of NCAM was analyzed. Under the basal conditions, neither JNK inhibitor nor the p38 inhibitor affected the mRNA and protein expression levels of NCAM (Fig. 5E). However, under oligomycin treatment, the p38 inhibitor SB202190 completely abolished the increases in the mRNA and protein expression levels of NCAM, while the JNK inhibitor SP600125 had no effect (Fig. 5F). Thus, up-regulation of NCAM under metabolic stress was revealed to be mediated by the activation of p38.

To determine the protective role of endogenous NCAM against oligomycin-induced metabolic stress, primary rat cardiac myocytes transfected with control-siRNA or NCAM-siRNA vector were treated with oligomycin and the survival rate was evaluated by MTT assay and a two-color fluorescence cell viability assay. As shown in Fig. 5G and Fig.

5H, both assays confirmed that knockdown of NCAM resulted in a significant reduction in survival rates following oligomycin treatment in primary rat cardiac myocytes.

These results suggested that expression of NCAM were enhanced and played a protective role in oligomycin-induced metabolic stress in primary rat neonatal cardiac myocytes.

*3.6. Signal transduction and protective role of NCAM mimetic peptide P2d*

Next, the downstream signaling of NCAM was evaluated in primary rat cardiac myocytes. AKT and ERK have been demonstrated to be the major downstream pathway elements in NCAM-induced signaling, and activation of these signaling pathways via NCAM has been reported to lead to cell survival effects in neuronal cells [14-16]. Therefore, the activation level of AKT and ERK was analyzed. As shown in Fig. 6A and 6B, it was found that the level of phosphorylated AKT was significantly reduced when NCAM was knocked down, whereas phosphorylated ERK levels remained unchanged, suggesting that NCAM was involved in AKT-mediated signaling. To further explore the NCAM-mediated signaling in cardiac myocytes, the effect of stimulation of NCAM was also analyzed using NCAM mimetic peptide P2d. P2d was synthesized as a dendrimer composed of four monomers corresponding to a 12-amino-acid sequence (GRILARGEIN

FK) in the second immunoglobulin (Ig)-like module of NCAM [22]. As shown in Fig. 6B, treatment with P2d at concentrations of 20μg/ml and 50μg/ml for 24 h activated AKT, whereas treatment with low concentration of P2d (5μg/ml) or with its scrambled form scrP2d (NLFEKGRRAIGI) (5-50μg/m) did not. Neither peptide activated ERK. Moreover, P2d protected cardiac myocytes from cell shrinkage during oligomycin treatment (Fig. 6C). An MTT assay was performed following treatment with 0.1μM oligomycin for 48 h in the presence of scrP2d or P2d at the indicated concentrations, and the results showed that P2d, but not scrP2d, reduced the rate of cell death at concentrations of 20μg/ml and 50μg/ml (Fig. 6D). To determine whether activation of AKT mediated the protective role of P2d, the effect of LY-294002 (10 μM) on cell survival was analyzed. It was found that LY-294002 completely abolished the cell survival effect of P2d (Fig. 6E). Furthermore, overexpression of the dominant negative form of AKT also eliminated the protective effect of P2d against oligomycin treatment (Fig. 6F). Taken together, these results indicated that the survival effect of P2d depended on the PI3K-AKT pathway.

## 4. Discussion

It is known that the failing heart expresses various adaptation proteins that work to protect the heart from injury [7-10]. Such factors can be used as biomarkers or therapeutic targets for heart failure. Among these, membrane proteins are easily accessible to exogenous drugs and are thus the preferred targets for drug development. The failing heart is characterized by alterations in energy metabolism, including mitochondrial dysfunction [1-6]. Oligomycin inhibits mitochondrial function by blocking $F_0F_1$ ATP synthase, leading to reduced ATP content. After the removal of oligomycin-containing medium and replacement with complete growth medium, the residual cells could be grown for further analyses. Thus, functional screening in combination with an SST method, which is a general strategy for cloning secreted proteins and type I membrane proteins, was set up to search for the genes that encode membrane proteins and are up-regulated by oligomycin treatment.

Through this approach, several genes encoding secreted and membrane proteins were identified. One of these genes was plasminogen activator inhibitor-1 (PAI-1) known to be up-regulated under the hypoxic condition [23], which supported the feasibility and

usefulness of our functional screening method.

In the present study, NCAM was identified as being up-regulated by oligomycin treatment in cardiac myocytes. It was also observed that NCAM was up-regulated in a mouse MI model. This was similar to the previous reports demonstrating the up-regulation of NCAM in ischemic cardiomyopathy [24]. NCAM was also found to be extensively up-regulated during the remodeling period of hypertrophy to heart failure in a Dahl salt-sensitive rat model. In particular, the expression pattern of NCAM in hypertensive hearts was impressive; NCAM was not expressed on the subepicardial side but was expressed strongly in the subendocardium area. These lesions are known to suffer readily from relative ischemia and metabolic stress and tend to develop fibrotic changes [25]. Indeed, strong expression of NCAM was found surrounding the fibrotic area.

Previous reports demonstrated that myocardial NCAM immunostaining was displayed from embryonic day E12 in the heart and increased up until postnatal day 1 and then declined rapidly thereafter [26]. Similarly, the present study found that immunostaining of NCAM was very scarce in normal adult hearts and restricted to the intercalated disks. Therefore, re-expression of NCAM under metabolic stress may be regarded as the reactivation of the fetal gene program, observed in the hemodynamically or metabolically

stressed heart, such as ANF re-expression, myosin heavy chain gene isoform switches, and GLUT isoform switches [27] and may be a sensitive marker for these conditions.

To investigate the pathways associated with NCAM induction in response to metabolic stress, the activation of stress-regulated MAP kinases was examined. It was found that p38 was rapidly activated by oligomycin treatment and blockage of p38 abolished the induction of NCAM expression. This is the same as with another neural cell adhesion molecule, contactin1, which was also reported to be induced by the p38 MAPK-dependent pathway [28]. p38 was reported to be involved in pathophysiology of ischemic and hypertensive heart disease [29, 30]. Thus, it is likely that expression of NCAM in MI and hypertensive hearts is also dependent on p38 activation.

The function of NCAM has been studied intensively in neuronal cells and has been shown to be involved in various biological process including cell migration, survival, and neuronal development. NCAM also has been shown to induce the activation of ERK and is anti-apoptotic via activation of the PI3K-AKT pathway in neurons [14, 16, 31]. In the present experiments with cardiac myocytes, it was shown that NCAM played a significant role in cell growth and survival under metabolic stress. Moreover, while basal ERK

activation did not change, NCAM-siRNA reduced AKT phosphorylation levels, suggesting that this pathway might be involved with the protective function of NCAM.

To further explore this signaling pathway, the effect of stimulation of NCAM was examined. Recently, by means of combinatorial chemistry and based on the unraveling of the structure of NCAM, a number of peptides that mimic NCAM homophilic binding have been developed [32, 33]. The P2 peptide, GRILARGEINFK, is a conserved sequence fragment of NCAM derived from the second Ig module, which represents the natural binding partner of the first Ig module of NCAM. The dendrimeric form of P2 (P2d) has been shown to bind NCAM IgI with an apparent Kd of 4.7 μM [22]. Thus, P2d has a mimetic function of NCAM homophilic binding. The effects of P2d have been examined in primary cerebellar and dopaminergic neurons, and it promotes neutrite outgrowth and protects against neuronal cell death [31, 34]. Here, it was demonstrated that P2d peptide also had a cardioprotective effect against metabolic stress via the PI3K-AKT pathway.

There are several possible mechanisms by which activation of NCAM can lead to activation of AKT. One possible mechanism involves FAK which is phosphorylated upon binding to the activated NCAM-Fyn complex [35]. PI3K has been shown to bind via the SH-2 domain of the p85 subunit to phosphorylated FAK, and this binding leads to

activation of PI3K and AKT [36]. Since activation of PI3K and AKT by phosphorylated FAK has been shown to protect cardiac myocytes from cell death under glucose deprivation, this pathway may be involved in NCAM mediated signaling and protection [37]. Another possible mechanism involves the FGFR which is activated upon homophilic NCAM-binding [38]. The FGFR has been shown to induce PI3K and AKT activation through recruitment of multiple docking proteins [39]. Thus, NCAM mediated activation of FGFR may induce the protective effect.

In conclusion, NCAM is specifically up-regulated in stressed cardiomyocytes, and augmentation of this signal improved cardiomyocyte survival through PI3K-AKT activation. Enhancement of NCAM-signaling by synthetic peptides may provide a novel strategy for heart failure therapy.

## Acknowledgements

We thank Naoya Sowa for excellent technical help.

## Sources of Funding

This study was supported in part by grants from the Ministry of Education, Culture, Sports, Science, and Technology (MEXT) of Japan to K. Ono, T. Kita, and T. Kimura.

## Figure legend

**Fig. 1.** Overview of the experimental procedure. (A) Measurement of cellular ATP concentration. H9C2 cells were treated with oligomycin (20 μM) for 48h. ATP concentration of untreated cells were set as 100%. Values are means±SEM, n=3. * P<0.01 n=3. (B) Overview of the experimental procedure. After U3Ceo retroviral infection, proviral integration into the introns of expressed genes results in splicing of upstream exons to the CD2/Neo gene. G418-resistant cells were treated with an FITC-conjugated monoclonal anti-CD2 antibody. CD2 expression was estimated by flow cytometry and CD2-negative cells were collected ($1^{st}$ sorting, Figure1-B, red) and expanded for oligomycin treatment. After treatment with oligomycin (20 μM) for 48h, the cells were collected again and analyzed for CD2 expression. In this step, CD2-positive cells were sorted and expanded to form single clones. ($2^{nd}$ sorting, Figure1-B, blue ). Samples from each clone were collected and analyzed for identification of the inserted genes by 5' rapid amplification of cDNA ends (5'-RACE, see Materials and Methods). (C) The junctional sequence of the fused cDNA in one of the clones obtained. SS; Signal sequence, SD; splicing donor, SA; splicing acceptor. (D) Cell surface CD2 levels of an untreated clone left (control) or treated with oligomycin (20 μM) for 48 h. The FITC level analyzed in cells

without FITC-conjugated monoclonal anti-CD2 antibody was set as a negative control. (E) The FITC level of cells treated with various concentrations and for various time periods. Values are means±SEM from at least three experiments. *P<0.01 vs control, **P<0.001 vs control. (F) and (G) Expression levels of NCAM mRNA (F) and protein (G) in H9C2 cells treated with oligomycin (20 μM) were examined by real-time PCR and western blotting analyses. β-actin is shown as a loading control. Values are means±SEM from at least three experiments. *P<0.01 vs. control;

**Fig. 2.** NCAM is up-regulated in mouse MI model. (A) Expression levels of NCAM in sham-operated (n=3) and MI mice (n=4) were determined by real-time PCR analyses. Apex area in MI mouse indicates infarcted area and septal area in MI mouse indicates non-infacted area. Values are means±SEM, *P<0.01, **P<0.001. (B)-(G) Immunohistochemical staining of NCAM in control and infarcted mice. (B) and (C) sham-operated mouse. (D)-(F) MI-operated mouse (day7). (E) infarcted area. (F) remote area. (G) infarct area of MI-operated mouse (12 months).

**Fig. 3.** NCAM is up-regulated in a rat model of hypertension-induced heart failure. (A)

ANF expression levels in the LV of DS rats at LVH and CHF stages were determined by real-time PCR analyses. Values represent arbitrary units (the 11W control values were set at 1.0). Values are means ± SEM, *P<0.01, **P<0.001. (B)-(M) Immunohistochemical staining of NCAM in DS rats. (B) and (C) 11 weeks LS (control). (D)-(J) 11 weeks HS (LVH). (H) Cross-section of LV in LVH rat. (I) and (J) Sequential section of LV in LVH rat. (I) Masson Trichrome stain. (J) NCAM staining. (K) and (L) 17 weeks HS (CHF). (M) 17 weeks LS (control). (N) NCAM mRNA level in the LV of DS rats at LVH and CHF periods were determined by real time PCR analyses. 11 weeks control, 11 weeks LVH, and 17 weeks control; n=6, 17 weeks CHF; n=7. Values represent arbitrary units (the 11W control values were set at 1.0). Values are means ± SEM, *P<0.001.

(O) Western blotting analyses of NCAM in the LV of DS rats in the LVH and CHF periods. GAPDH is shown as a loading control.

**Fig. 4.** Knockdown of NCAM reduced the survival rate after oligomycin treatment in H9C2 cells. (A) Effect of knockdown of NCAM with NCAM-siRNA in H9C2 cells. β-actin is shown as a loading control. (B) Effect of knockdown of NCAM on the proliferation rate of H9C2 cells. Seventy-two hours after transfection with control-siRNA or NCAM-siRNA,

H9C2 cells were plated as $1.2\times10^4$/mL and cell proliferation was assessed. Values are means ± SEM , *P<0.05 relative to siCTRL. n=3 (C) Knockdown of NCAM decreased the BrdU uptake in H9C2. Values are means ± SEM *P<0.0001 from 3 independent experiments in 5-6 wells. (D) Phase-contrast image of H9C2 cells transfected with control-siRNA or NCAM-siRNA with or without treatment with oligomycin (20 μM) for 48h. (×200) (E) Viable cells transduced with control-siRNA or NCAM-siRNA with or without treatment with oligomycin (20 μM) for 48h was assessed by MTT assay. The MTT level of untreated H9C2 cells transduced with control-siRNA was set as 1.0. Values are means ± SEM of three independent experiments. *P<0.01, **P<0.001 (F) and (G) Live and dead cells in each condition were determined using a two-color fluorescence cell viability assay as described in the materials and methods. (F) Representative images of a two-color fluorescence cell viability assay (green; viable cells, red; dead cells ×100). (G) The main graph shows the actual numbers of live (green) and dead (red) cells per view fields. Live cells (green) / total cells (green + red) × 100% in each group was calculated and used for cell viability. The result was shown in the inset. Values are means ± SEM, *P<0.001

**Fig. 5.** NCAM is up-regulated under oligomycin-induced metabolic stress by the p38

MAPK dependent pathway and played a protective role in primary neonatal rat cardiac myocytes. (A) Measurement of cellular ATP concentration. Primary neonatal rat cardiac myocytes were treated with oligomycin (0.1 μM) for 48h. The ATP level of untreated cells were set as 100%. Values are means ± SEM, n=3, *P<0.001 (B) Oligomycin (0.1 μM) treatment activated p38 but not JNK. (C) The change in endogenous NCAM expression level in rat neonatal cardiac myocytes was analyzed by real-time PCR. Values are means ± SEM, n=3, *P<0.05 (D) Western blotting analyses of NCAM with or without oligomycin (0.1 μM) treatment for 48h. β-actin is shown as a loading control. The lower graph shows densitometry analyses. Values are means ± SEM, n=3, *P<0.001. (E) and (F) Effect of P38 inhibitor (SB202190, 10 μM) and JNK inhibitor (SP600125, 10 μM) on NCAM expression under the basal conditions (E) and oligomycin treatment (F) examined by real-time PCR and western blotting analyses. SB, SB202190; SP, SP600125; Values are means ± SEM, n=3, *P<0.01 vs control. (G) Viable cells transduced with control-siRNA or NCAM-siRNA with or without oligomycin (0.1 μM) treatment for 48h were assessed by MTT assay. *P<0.001, n=3 (H) Live and dead cells in each condition were determined using a two-color fluorescence cell viability assay. Left-hand pictures show representative fluorescence microscopic images (×100). Right-hand graph shows the result of cell viability

quantified by counting the number of viable (green) and dead (red) cells per experiment. * P<0.001

**Fig. 6.** NCAM is involved in AKT mediated signaling and NCAM mimetic peptide P2d has a protective effect against oligomycin-induced metabolic stress via the PI3K-AKT pathway. (A) Seventy-two hours after lentivirus infection, phospho-AKT(Ser473), total-AKT, phospho-ERK(p42/44), and total-ERK were analyzed by western blotting. The graph shows the results of densitometry analysis from three independent experiments. Mean ± SEM, *P<0.05 (B) Lysates from cardiac myocytes treated with scrP2d or P2d (5, 20, and 50 μg/mL) for 24 h were assessed for Akt and ERK activity. β-actin is shown as a loading control. (C) Phase-contrast image of cardiac myocytes following oligomycin (0.1 μM) treatment for 48h in the presence of vehicle, scrP2d or P2d (20 μg/mL). (D) MTT assay was performed following treatment with oligomycin (0.1 μM) for 48 h in the presence of scrP2d or P2d as indicated. Mean ± SEM from at least three experiments. **P<0.01 *P<0.001. (E) Treatment with LY-294002 (10 μM) abolished the cell survival effect of P2d. Mean ± SEM, n=6, *P<0.05, **P<0.01. (F) Overexpression of the dominant negative Akt eliminated the cell survival effect of P2d. vector; control empty vector, DN-AKT; dominant

negative AKT. Mean ± SEM, n=3, *P<0.001.

## References

[1] Neubauer S. The failing heart--an engine out of fuel. N Engl J Med 2007; 356: 1140-51.

[2] Stanley WC, Recchia FA, Lopaschuk GD. Myocardial substrate metabolism in the normal and failing heart. Physiol Rev 2005; 85: 1093-129.

[3] Ventura-Clapier R, Garnier A, Veksler V. Energy metabolism in heart failure. J Physiol 2004; 555: 1-13.

[4] Jarreta D, Orus J, Barrientos A, Miro O, Roig E, Heras M, et al. Mitochondrial function in heart muscle from patients with idiopathic dilated cardiomyopathy. Cardiovasc Res 2000; 45: 860-5.

[5] Marin-Garcia J, Goldenthal MJ, Moe GW. Mitochondrial pathology in cardiac failure. Cardiovasc Res 2001; 49: 17-26.

[6] Rosca MG, Vazquez EJ, Kerner J, Parland W, Chandler MP, Stanley W, et al. Cardiac mitochondria in heart failure: decrease in respirasomes and oxidative phosphorylation. Cardiovasc Res 2008; 80: 30-9.

[7] de Bold AJ, Borenstein HB, Veress AT, Sonnenberg H. A rapid and potent natriuretic response to intravenous injection of atrial myocardial extract in rats. Life Sci 1981; 28:

89-94.

[8] Funamoto M, Hishinuma S, Fujio Y, Matsuda Y, Kunisada K, Oh H, et al. Isolation and characterization of the murine cardiotrophin-1 gene: expression and norepinephrine-induced transcriptional activation. J Mol Cell Cardiol 2000; 32: 1275-84.

[9] Maekawa K, Sudoh T, Furusawa M, Minamino N, Kangawa K, Ohkubo H, et al. Cloning and sequence analysis of cDNA encoding a precursor for porcine brain natriuretic peptide. Biochem Biophys Res Commun 1988; 157: 410-6.

[10] Tsuruda T, Kato J, Kitamura K, Kuwasako K, Imamura T, Koiwaya Y, et al. Adrenomedullin: a possible autocrine or paracrine inhibitor of hypertrophy of cardiomyocytes. Hypertension 1998; 31: 505-10.

[11] Gebauer M, von Melchner H, Beckers T. Genomewide trapping of genes that encode secreted and transmembrane proteins repressed by oncogenic signaling. Genome Res 2001; 11: 1871-7.

[12] Doherty P, Ashton SV, Moore SE, Walsh FS. Morphoregulatory activities of NCAM and N-cadherin can be accounted for by G protein-dependent activation of L- and N-type neuronal Ca2+ channels. Cell 1991; 67: 21-33.

[13] Maness PF, Schachner M. Neural recognition molecules of the immunoglobulin

superfamily: signaling transducers of axon guidance and neuronal migration. Nat Neurosci 2007; 10: 19-26.

[14] Ditlevsen DK, Kohler LB, Pedersen MV, Risell M, Kolkova K, Meyer M, et al. The role of phosphatidylinositol 3-kinase in neural cell adhesion molecule-mediated neuronal differentiation and survival. J Neurochem 2003; 84: 546-56.

[15] Ditlevsen DK, Povlsen GK, Berezin V, Bock E. NCAM-induced intracellular signaling revisited. J Neurosci Res 2008; 86: 727-43.

[16] Walmod PS, Kolkova K, Berezin V, Bock E. Zippers make signals: NCAM-mediated molecular interactions and signal transduction. Neurochem Res 2004; 29: 2015-35.

[17] Hasegawa K, Meyers MB, Kitsis RN. Transcriptional coactivator p300 stimulates cell type-specific gene expression in cardiac myocytes. J Biol Chem 1997; 272: 20049-54.

[18] Fujio Y, Nguyen T, Wencker D, Kitsis RN, Walsh K. Akt promotes survival of cardiomyocytes in vitro and protects against ischemia-reperfusion injury in mouse heart. Circulation 2000; 101(6): 660-7.

[19] Inagaki K, Iwanaga Y, Sarai N, Onozawa Y, Takenaka H, Mochly-Rosen D, et al.

Tissue angiotensin II during progression or ventricular hypertrophy to heart failure in hypertensive rats; differential effects on PKC epsilon and PKC beta. J Mol Cell Cardiol 2002; 34: 1377-85.

[20] Iwanaga Y, Aoyama T, Kihara Y, Onozawa Y, Yoneda T, Sasayama S. Excessive activation of matrix metalloproteinases coincides with left ventricular remodeling during transition from hypertrophy to heart failure in hypertensive rats. J Am Coll Cardiol 2002; 39: 1384-91.

[21] Iwanaga Y, Kihara Y, Hasegawa K, Inagaki K, Yoneda T, Kaburagi S, et al. Cardiac endothelin-1 plays a critical role in the functional deterioration of left ventricles during the transition from compensatory hypertrophy to congestive heart failure in salt-sensitive hypertensive rats. Circulation 1998; 98: 2065-73.

[22] Soroka V, Kiryushko D, Novitskaya V, Ronn LC, Poulsen FM, Holm A, et al. Induction of neuronal differentiation by a peptide corresponding to the homophilic binding site of the second Ig module of the neural cell adhesion molecule. J Biol Chem 2002; 277: 24676-83.

[23] Kietzmann T, Roth U, Jungermann K. Induction of the plasminogen activator inhibitor-1 gene expression by mild hypoxia via a hypoxia response element binding the

hypoxia-inducible factor-1 in rat hepatocytes. Blood 1999; 94: 4177-85.

[24] Gattenlohner S, Waller C, Ertl G, Bultmann BD, Muller-Hermelink HK, Marx A. NCAM(CD56) and RUNX1(AML1) are up-regulated in human ischemic cardiomyopathy and a rat model of chronic cardiac ischemia. Am J Pathol 2003; 163: 1081-90.

[25] Sharov VG, Todor AV, Silverman N, Goldstein S, Sabbah HN. Abnormal mitochondrial respiration in failed human myocardium. J Mol Cell Cardiol 2000; 32: 2361-7.

[26] Wharton J, Gordon L, Walsh FS, Flanigan TP, Moore SE, Polak JM. Neural cell adhesion molecule (N-CAM) expression during cardiac development in the rat. Brain Res 1989; 483: 170-6.

[27] Rajabi M, Kassiotis C, Razeghi P, Taegtmeyer H. Return to the fetal gene program protects the stressed heart: a strong hypothesis. Heart Fail Rev 2007; 12: 331-43.

[28] Su JL, Yang PC, Shih JY, Yang CY, Wei LH, Hsieh CY, et al. The VEGF-C/Flt-4 axis promotes invasion and metastasis of cancer cells. Cancer Cell 2006; 9: 209-23.

[29] Li J, Miller EJ, Ninomiya-Tsuji J, Russell RR, 3rd, Young LH. AMP-activated protein kinase activates p38 mitogen-activated protein kinase by increasing recruitment of p38 MAPK to TAB1 in the ischemic heart. Circ Res 2005; 97: 872-9.

[30] Sugden PH, Clerk A. "Stress-responsive" mitogen-activated protein kinases (c-Jun N-terminal kinases and p38 mitogen-activated protein kinases) in the myocardium. Circ Res 1998; 83: 345-52.

[31] Pedersen MV, Kohler LB, Ditlevsen DK, Li S, Berezin V, Bock E. Neuritogenic and survival-promoting effects of the P2 peptide derived from a homophilic binding site in the neural cell adhesion molecule. J Neurosci Res. 2004; 75: 55-65.

[32] Berezin V, Bock E. NCAM mimetic peptides: Pharmacological and therapeutic potential. In: J Mol Neurosci; 2004: 33-9.

[33] Berezin V, Bock E. NCAM Mimetic Peptides: An Update. Neurochem Res 2008.

[34] Klementiev B, Novikova T, Korshunova I, Berezin V, Bock E. The NCAM-derived P2 peptide facilitates recovery of cognitive and motor function and ameliorates neuropathology following traumatic brain injury. Eur J Neurosci 2008; 27: 2885-96.

[35] Beggs HE, Baragona SC, Hemperly JJ, Maness PF. NCAM140 interacts with the focal adhesion kinase p125(fak) and the SRC-related tyrosine kinase p59(fyn). J Biol Chem 1997; 272: 8310-9.

[36] Chen HC, Appeddu PA, Isoda H, Guan JL. Phosphorylation of tyrosine 397 in focal adhesion kinase is required for binding phosphatidylinositol 3-kinase. J Biol Chem 1996;

271: 26329-34.

[37] Del Re DP, Miyamoto S, Brown JH. Focal adhesion kinase as a RhoA-activable signaling scaffold mediating Akt activation and cardiomyocyte protection. J Biol Chem 2008; 283: 35622-9.

[38] Kiselyov VV, Soroka V, Berezin V, Bock E. Structural biology of NCAM homophilic binding and activation of FGFR. J Neurochem 2005; 94: 1169-79.

[39] Ong SH, Hadari YR, Gotoh N, Guy GR, Schlessinger J, Lax I. Stimulation of phosphatidylinositol 3-kinase by fibroblast growth factor receptors is mediated by coordinated recruitment of multiple docking proteins. Proc Natl Acad Sci U S A 2001; 98: 6074-9.

# Fig. 1

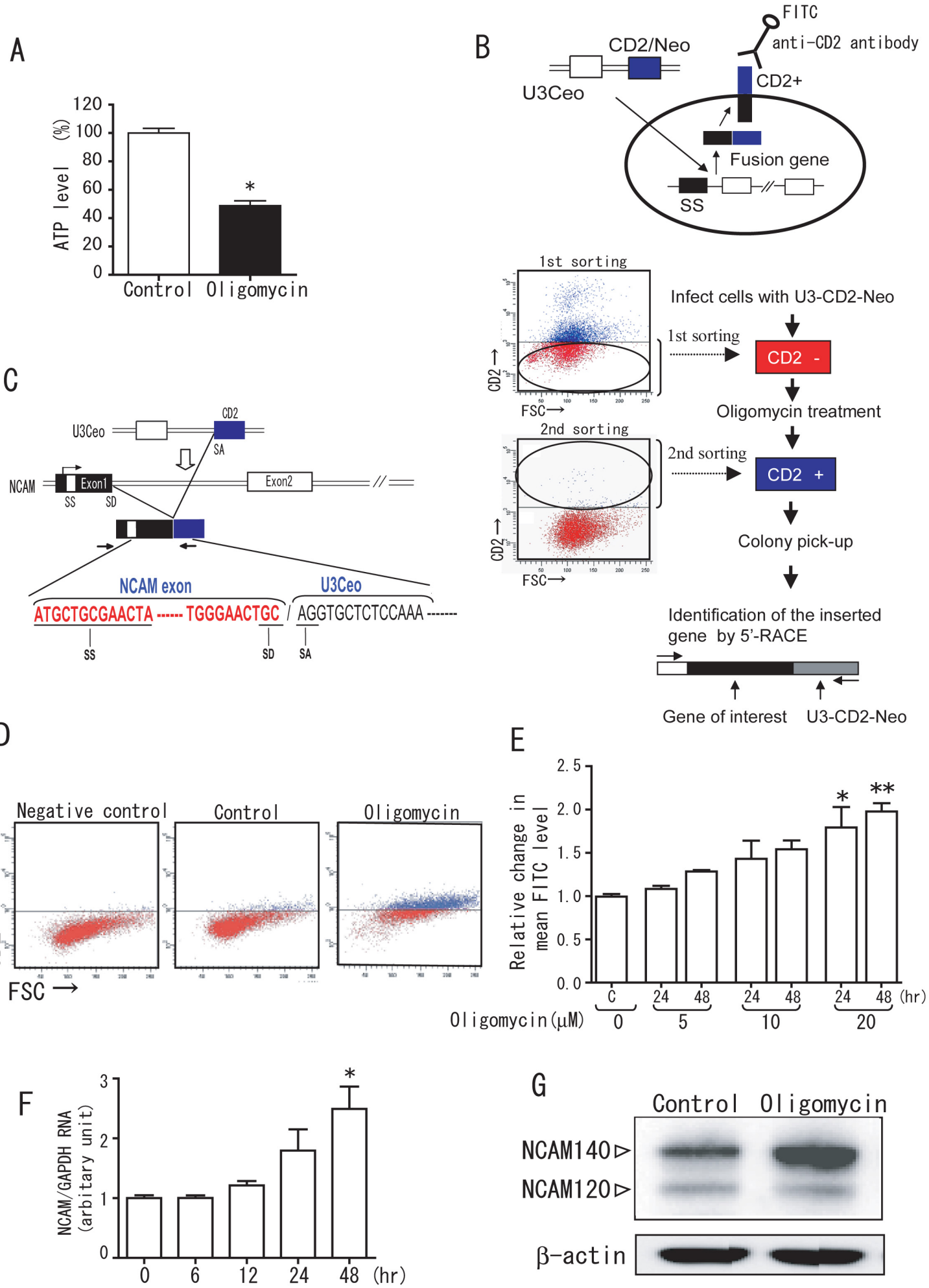

# Fig. 2

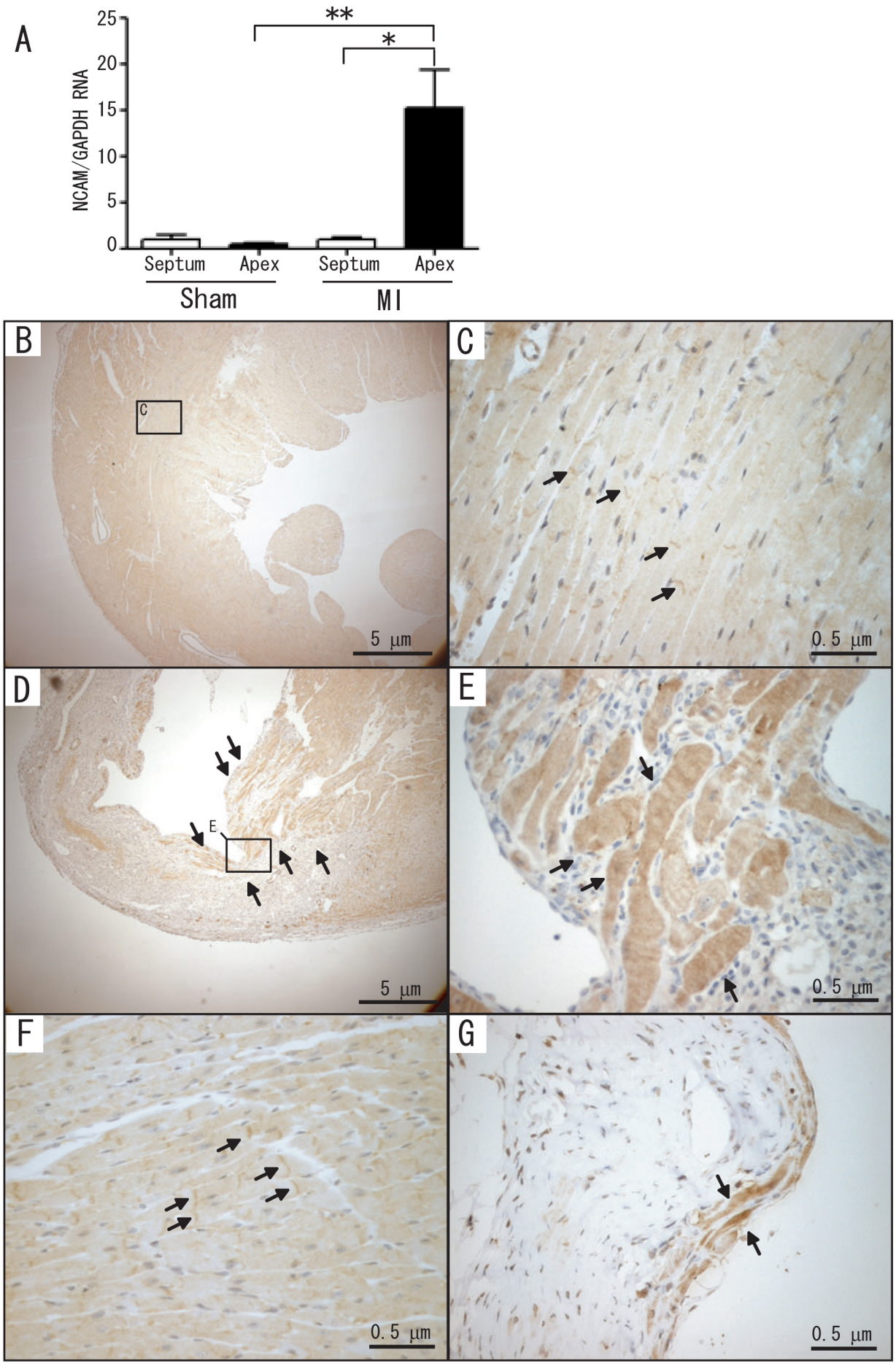

Fig. 3

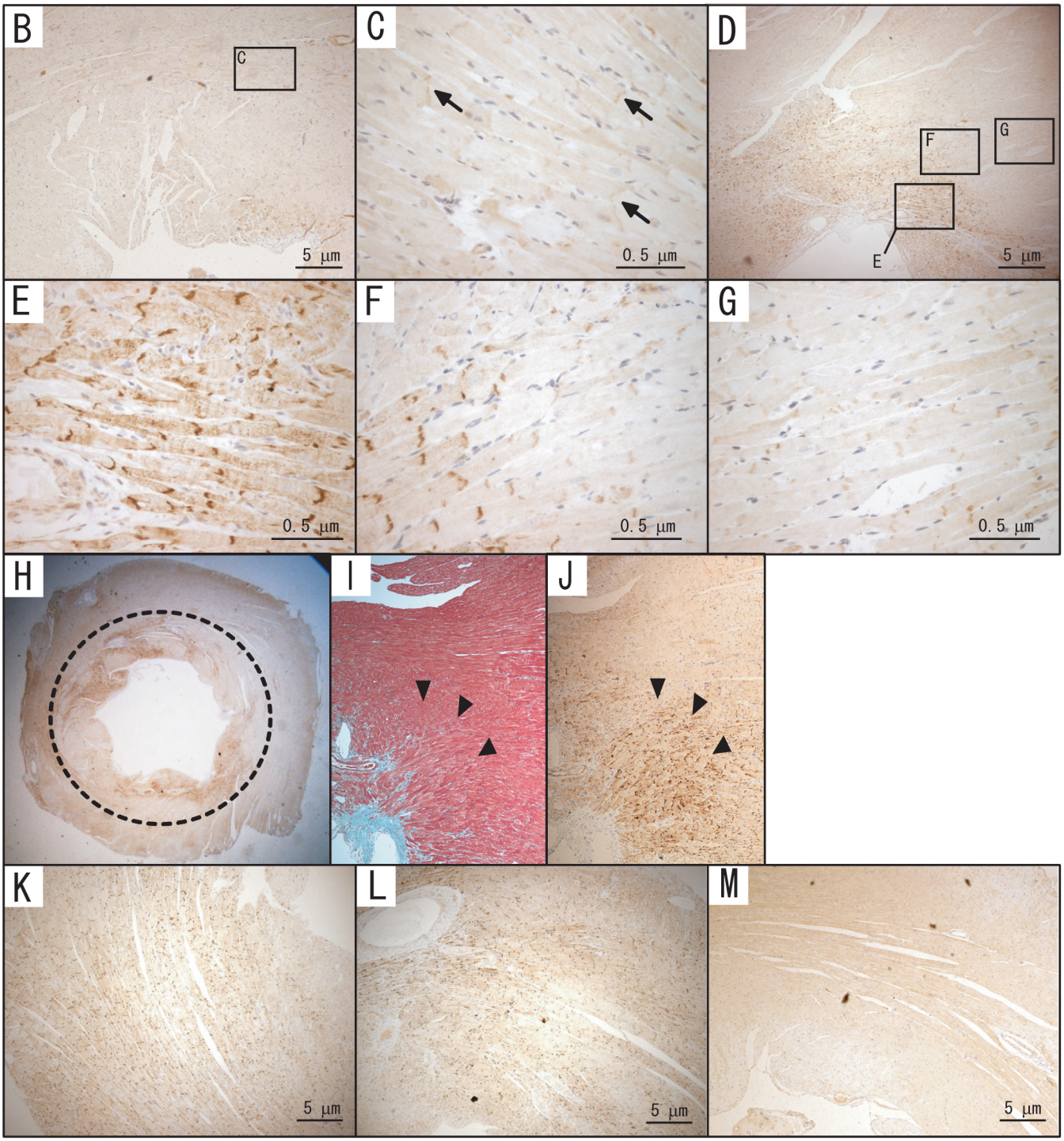

# Fig. 4

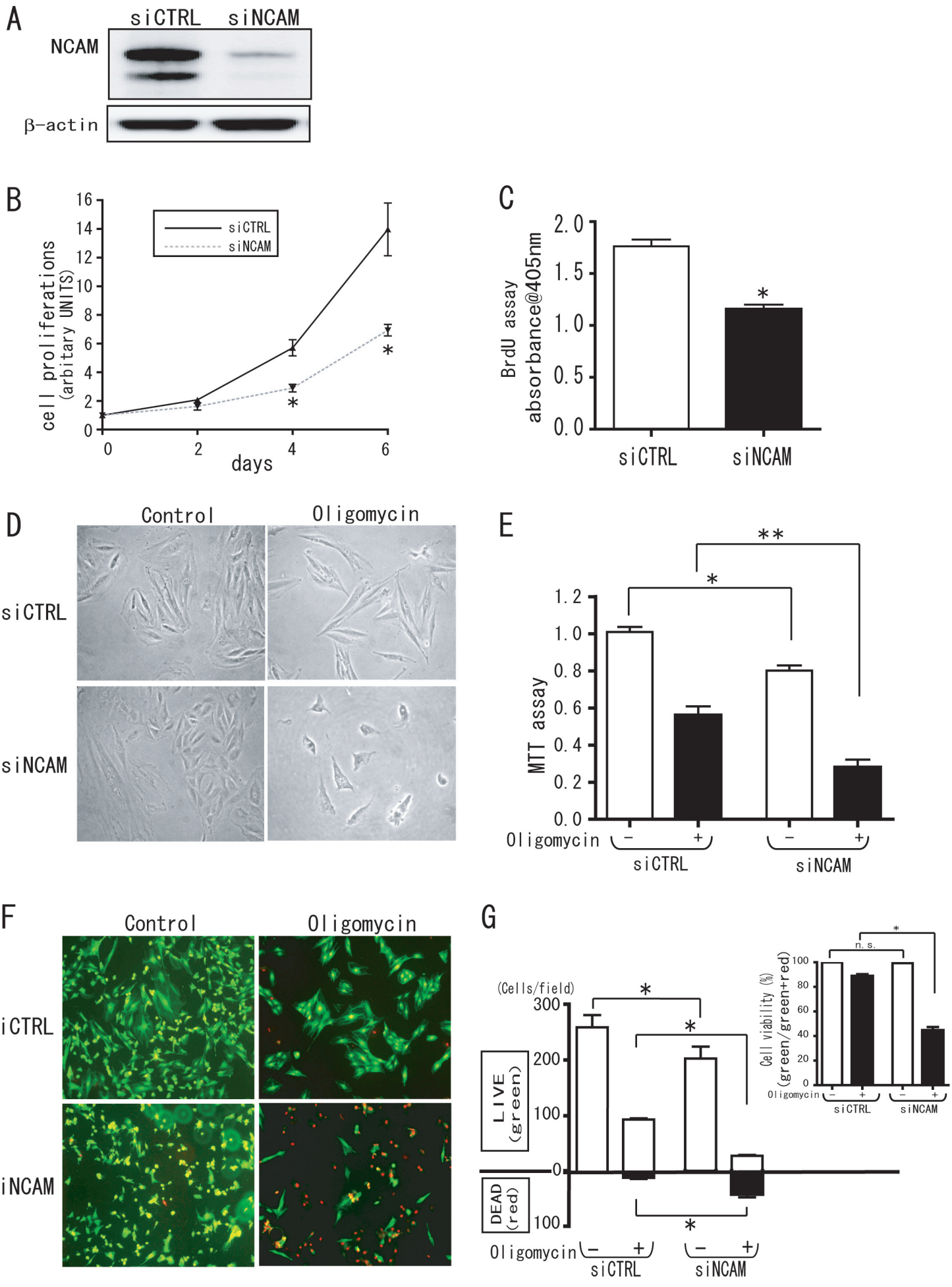

# Fig. 5

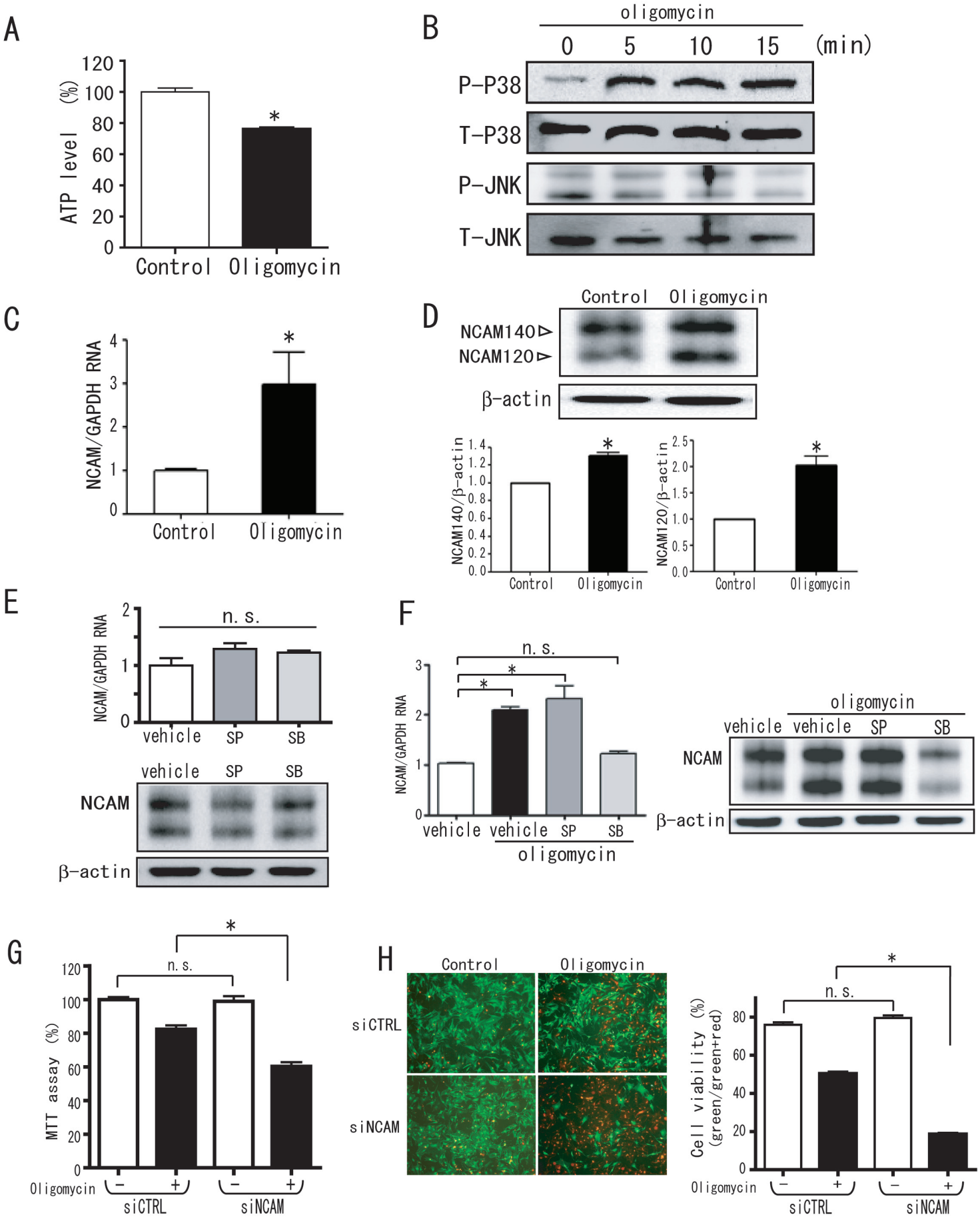

# Fig. 6